# Impact of Total Ionizing Dose on the alpha-Soft Error Rate in FDSOI 28 nm SRAMs

Soilihi Moindje, Daniela Munteanu, Jean-Luc Autran, Victor Malherbe, Gilles Gasiot, Philippe Roche

# Impact of Total Ionizing Dose on the alpha-Soft Error Rate in FDSOI 28 nm SRAMs

S. Moindjie[a], D. Munteanu[a], J.L. Autran[a,*], V. Malherbe[b], G. Gasiot[b], P. Roche[b]

[a]*Aix-Marseille Univ., CNRS, IM2NP (UMR 7334), 13397 Marseille Cedex 20, France*
[b]*STMicroelectronics, 850 rue Jean Monnet, 38926 Crolles Cedex, France*

**Abstract**

Synergy effect of total ionizing dose (TID) on alpha-soft error rate (α-SER) in FDSOI 28nm SRAM has been experimentally characterized using a dedicated setup combining alpha-particle irradiation ($^{241}$Am solid source) in vacuum chamber and 10 keV X-ray irradiation. Modeling and simulation have been used to link transistor threshold voltage variations to SRAM cell stability in terms of static noise margin (SNM), critical charge ($Q_{crit}$) and finally estimated SER, in good agreement with experimental results.

## 1. Introduction

Synergy effects between total ionizing dose (TID) and single event effects (SEE) on devices and circuits are fundamental to apprehend electronic reliability in various environments, like space, accelerators or future power fusion reactors. In such complex radiation environments, equipments or payloads are or will be subjected to both TID and SEE at the same time, which leads to combined effects on the electronics [1-3]. However, radiation qualification procedures often perform separate characterizations and, consequently, are not able to catch the underlying physical mechanisms responsible of dose-enhancement SEE sensitivity or other effects.

In this work, we experimentally investigate synergy effects between TID and alpha-particle SER in FDSOI 28nm SRAM combining the use of a $^{241}$Am solid source and 10 keV X-ray irradiation machine to successively degrade and evaluate the circuit response. The key objective of this study is to model and simulate such effects, step by step, from individual transistor threshold voltage variations to SRAM SER, evaluating the cell stability in terms of static noise margin (SNM), critical charge ($Q_{crit}$) and finally soft error rate. The paper is organized in two main parts: we describe in Section 2 the circuit under test and the irradiation test setups, as well as the experimental results. In Section 3, modelling and simulation aspects are presented and used to reproduce experimental data.

## 2. Experiments

### *2.1. SRAM test vehicle*

In this study, we used a dedicated test vehicle (ANYA_D) manufactured by STMicroelectronics using a commercial ultra-thin body and buried oxide (UTBB) fully-depleted silicon-on insulator (FDSOI) CMOS 28 nm technology. The UTBB-FDSOI uses a 28 nm high-κ metal-gate, the silicon layer is 7 nm thick on top of an ultra-thin buried oxide of 25 nm. Details can be found in [4-6], including process description, electrical performances and single event test results for the terrestrial radiation environment (alphas and neutrons). ANYA_D embeds several SRAMs cuts of various densities and power features (Fig. 1 left). For the purposes of the study, we performed all of our measurements on a 3 Mbit single-port high-density (SPHD) SRAM cut powered at $V_{DD}$ = 1 V. The circuit schematic of the corresponding SPHD SRAM cell is given in Fig. 1 (right).

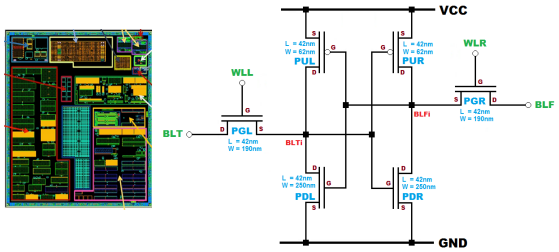


Fig. 1. GDS view of ANYA_D test vehicle (left) and circuit schematic of the single-port high-density (SPHD) SRAM cell.

* Corresponding author. jean-luc.autran@univ-amu.fr

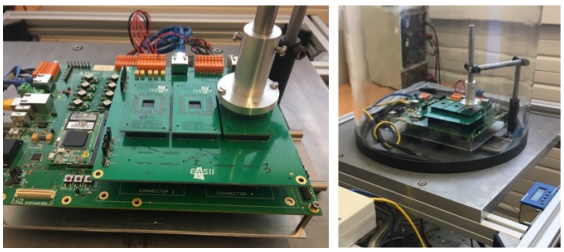

Fig. 2. Alpha-particle irradiation setup using a $^{214}$Am solid source (4 kBq in 2π sr) and a vacuum bell jar. All of the circuit connections go through vacuum connectors, allowing real-time measurements during irradiation.

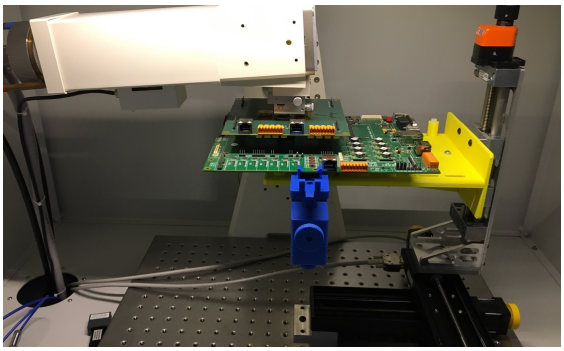

Fig. 3. X-ray irradiation setup using a 10 keV X-ray tube with a tungsten cathode.

*2.2. Experimental setups*

For the purpose of the study of synergy effects, we designed, constructed and operated a complete experimental setup for both α-SER and TID measurements. This setup consist of a vacuum chamber (bell jar) in which a circuit tester can be operated under a primary vacuum ($10^{-2}$ mbar), in order to maintain the energy of alpha-particles emitted by the source at the level of the entry face of the circuit. The circuit tester is fully connected to the exterior via vacuum connectors. Fig. 2 shows the experimental setup in irradiation configuration with an $^{Am}$241 solid source placed in front of a decapsulated ANYA_D circuit, ready to characterize. Setup of Fig. 2 was used to performed the α-SER characterization of the circuit under test. After this measurement step, the tester itself with the circuit was moved to the X-ray irradiation setup (Fig. 3) for irradiation at a dose rate of 100 rad(Si)/s. Repeating the cycle (α-SER measurement + X-ray irradiation) for different values of the TID allows us to characterize synergy effects between SER and TID in the range from 0 to 128 krad(Si).

*2.2. α-SER versus TID experimental results*

Fig. 4 shows the cumulated number of bit flips detected during α-irradiation as a function of measurement time before (fresh) and after X-ray

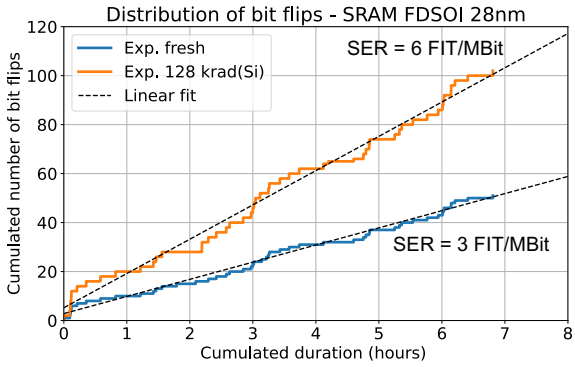


Fig. 4. Cumulated number of bit flips in 3 Mbit SRAM cut ($V_{DD}$ = 1 V) as a function of the α-irradiation time before (fresh) and after 128 krad(Si) X-ray irradiation of the circuit. The corresponding SER (FIT/Mbit) is calculated for an α-emissivity of $10^{-3}$ α/cm$^2$/h. For industrial confidentiality reason, all SER results have been normalized by a common arbitrary scaling factor.

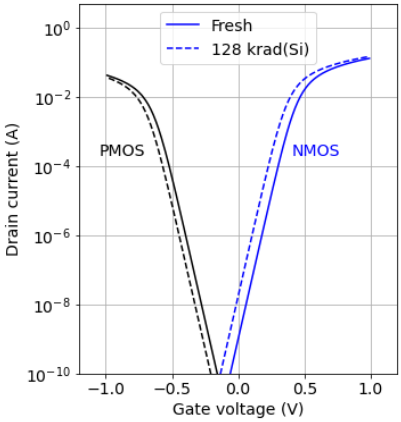


Fig. 5. $I_D(V_G)$ characteristics before (fresh) and after 10 keV X-ray irradiation at 128 krad(Si) for both NMOS and PMOS transistors (L = 42 nm, W = 1 µm).

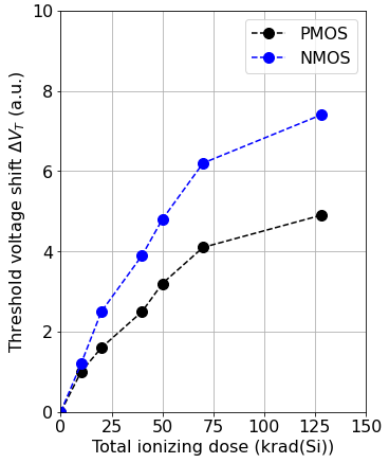


Fig. 6. Negative threshold voltage shifts versus TID extracted from $I_D(V_G)$ curves for both NMOS and PMOS transistors. For industrial confidentiality reason, all values have been normalized by a common arbitrary scaling factor.

irradiation that corresponds to the maximum dose of 128 krad(Si) for which the circuit is fully functional. Note the surprisingly long duration of the experiments (up to 7 hours) for such accelerated tests using a source with 4 kBq of activity: this is due to the relative immunity of FDSOI architectures to single events, characterized by very low SER values, reported in Fig. 4. The two distribution slopes are precisely linked to the α-SER: after 128 krad(Si), the slope (and thus the SER) is quasi twice that of the distribution before irradiation, demonstrating the TID synergy effect on the circuit SER. In the following, our objective is to step-by-step retrieve by simulation and confirm this measured SER from the TID response of both NMOS and PMOS transistors, elements of the SRAM cell.

*2.3. TID characterization of individual transistors*

In complement to SER versus TID experiments, we performed electrical characterization of individual transistors for the extraction of the threshold voltage shift as a function of TID. Fig. 5 shows the $I_D(V_G)$ characteristics before irradiation and after 128 krad(Si) for both NMOS and PMOS individual transistors. $\Delta V_T$ is negative since the radiation-induced trapped charges are mainly positive whatever the type of the transistor [7]. $\Delta V_T$ versus TID (Fig. 6) are also more important in absolute value for NMOS than for PMOS. The latter appear to be less TID-sensitive than NMOS, as already shown [7].

## 3. Modelling and simulation

*3.1 Transistor and SRAM modelling*

We implemented in C++ the UTSOI model (v1.1.4) developed by the CEA-LETI (and initially in the form of Verilog-A(MS) source code) for ultra-thin fully depleted SOI MOSFET [8]. The model library was used in our standalone SRAM cell simulator [9] for time-domain transient simulation and for the determination of the static noise margin (SNM) and critical charge $Q_{crit}$, as shown in the following.

*3.2. Static noise margin*

Fig. 7 shows the computed SRAM "butterfly" curves before and after several doses, up to 128 krad(Si). The effect of the dose on the reduction of the static noise margin, taken into account via the $\Delta V_T$ values for both PMOS and NMOS transistors of the SRAM cell, is clearly visible. For memory, the SNM is defined as the side length of the largest square that can be fitted inside the lobes of the "butterfly" curve. Fig. 7 evidences the closing of the curves, quantified in Fig. 8 in terms of SNM values. At 128 krad(Si), SNM is reduced to about 20% with respect to the value before irradiation.

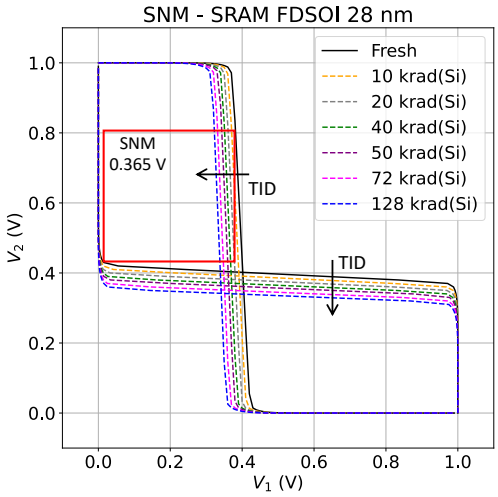


Fig. 7. Simulated SRAM cell "butterfly" curves before and after irradiation at several TID values. SNM is graphically extracted here for the curve before irradiation (fresh).

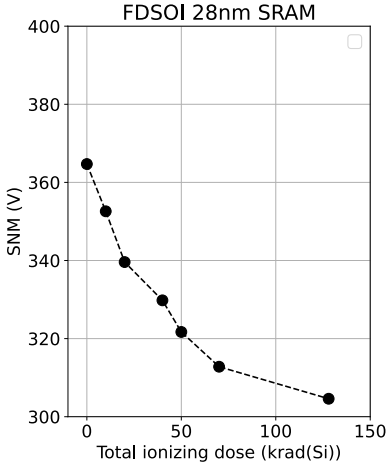


Fig. 8. SNM versus TID for the FDSOI 28 nm SPHD SRAM cell defined in Fig. 1 (right) and extracted from numerical simulation shown in Fig. 7.

*3.3. Critical charge*

This decrease in stability of the SRAM cell, evidenced by the SNM reduction, has a direct impact on its susceptibility to single events. For simulating such events at circuit level, we used a double exponential current transient pulse $i_{inj}(t)$ injected on the struck node during the transient simulation [10]:

$$i_{inj}(t) = \frac{Q}{t_f - t_r}\left[exp(-t/t_f) - exp(-t/t_r)\right] \quad (1)$$

where $Q$ is the collected charge on the struck node (i.e., the integral of the pulse), $t_r$ is the rising time constant, and $t_f$ is the falling time constant. Slowly varying Q around the stability point of the SRAM cell allows us to determine the critical charge for a given TID value, as illustrated in Fig. 9 for the fresh cell.

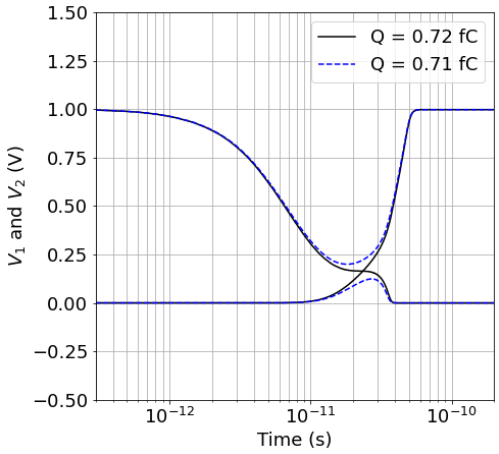


Fig. 9. Transient simulation of the SRAM cell (before irradiation) subjected to a particle strike mimicked by (1) with two values of Q. $V_1$ and $V_2$ corresponds to the potentials of the two storage nodes of the cell.

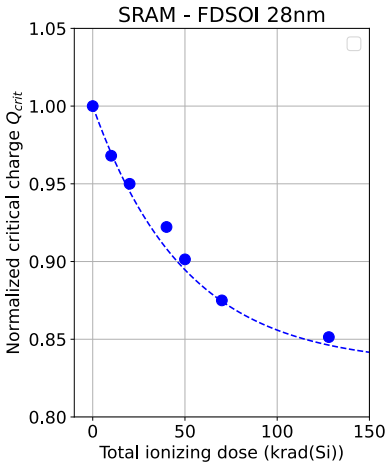


Fig. 10. Critical charge versus TID extracted from transient simulation considering a double exponential current pulse.

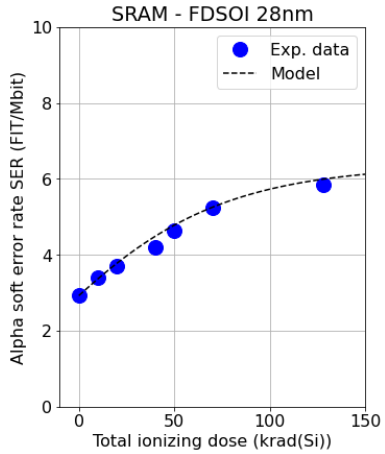


Fig. 11. Alpha soft error rate versus TID for the FDSOI 28 nm SPHD SRAM as deduced from experimental data of Fig. 4 and from Eq. (2) using $Q_{crit}$ values of Fig. 10.

*3.4. Soft error rate*

Fig. 10 shows the decrease of $Q_{crit}$ with TID, well described by an exponential law with a unique parameter $\lambda = 0.02$ krad(Si)$^{-1}$. This decrease of $Q_{crit}$ leads to an increase of the SER with TID, illustrated in Fig. 11, predicted by the Hazucha and Svensson's equation for the SER [11]:

$$SER = \kappa \cdot F \cdot A_S \cdot exp\left(-\frac{Q_{crit}}{Q_S}\right) \qquad (2)$$

The final paper will detail the evaluation of parameters $\kappa$ an d $Q_S$ for FDSOI devices and the SER evaluation that allowed us to retrieve by calculation the experimental values, as shown in Fig. 11.

## Acknowledgements

The financial support of the French DGA directorate (DGA/RAPID #162906056) is gratefully acknowledged. The authors also thank M. Naceur and the technical staff of EASII-IC (Grenoble) for the development of electronic cards and testers.

## References

[1] E. G. Stassinopoulos, G. J. Brucker, O. Van Gunten and H. S. Kim, "Variation in SEU sensitivity of dose-imprinted CMOS SRAMs," in IEEE Transactions on Nuclear Science, vol. 36, no. 6, pp. 2330-2338, Dec. 1989.

[2] L. Salvy *et al.*, "Total ionizing dose influence on the single event effect sensitivity of active EEE components," *2016 16th European Conference on Radiation and Its Effects on Components and Systems (RADECS)*, Bremen, Germany, 2016.

[3] J. Li et al., "Effects of total ionizing dose on transient ionizing radiation upset sensitivity of 40–180 nm SRAMs", AIP Advances 12, 015026 (2022).

[4] N. Planes, et al., "28nm FDSOI Technology Platform for High-Speed Low-Voltage Digital Applications," p333, VLSI 2012.

[5] P. Roche, J.L. Autran, G. Gasiot, D. Munteanu, "Technology Downscaling Worsening Radiation Effects in Bulk: SOI to the Rescue," Invited paper at IEEE International Electron Devices Meeting (IEDM), Dec. 2013 , pp. 31.1.1 - 31.1.4.

[6] G. Gasiot *et al.,* "SER/SEL performances of SRAMs in UTBB FDSOI28 and comparisons with PDSOI and BULK counterparts," 2014 IEEE International Reliability Physics Symposium, Waikoloa, HI, USA, 2014, pp. SE.6.1-SE.6.5.

[7] M. Gaillardin *et al.*, "Total Ionizing Dose Effects Mitigation Strategy for Nanoscaled FDSOI Technologies," in *IEEE Transactions on Nuclear Science*, vol. 61, no. 6, pp. 3023-3029, Dec. 2014.

[8] https://www.leti-cea.fr/cea-tech/leti/Documents/UTSOI/Model_Description_UTSOI_v11 3_light.pdf

[9] J.L. Autran et al., "Charge Collection Physical Modeling for Soft Error Rate Computational Simulation in Digital Circuits," in *Modeling and Simulation in Engineering Sciences*, N. Sher Akbar, O. Anwar Beg. (Edts.), IntechOpen, pp.115-137, 2016.

[10] J.L. Autran, D. Munteanu. *Soft errors: from particles to circuits.* Boca Raton: CRC Press, 2015.

[11] P. Hazucha and C. Svensson, "Impact of CMOS Technology Scaling on the Atmospheric Neutron Soft Error Rate," IEEE Trans. Nucl. Sci., vol. 47, no. 6, pp. 2586-2594, Dec. 2000.